ATLAS NOTE

October 2, 2007

Impacts of misalignment effects on the Muon Spectrometer Performance

N. Benekos [(a)1], L. Chevalier [(b)], J.F. Laporte [(c)], M. Schott [(d)2],

(a) Max Planck Institut für Physik, München, Germany
Föhringer Ring 6, D-80805 München, Germany
(b) CEA Saclay DAPNIA, 91191 Gif-sur-Yvette, Paris, France
(c) Ludwig-Maximilians-Universität München
Am Coulombwall 1,
D-85748 Garching, Germany

Abstract

The ATLAS detector, currently being installed at CERN, is designed to exploit the full potential of the LHC. Starting in 2008, it will identify and provide highly accurate energy and momentum measurements of particles emerging from the LHC proton-proton collisions with a centre-of-mass energy at 14 TeV. High-momentum muons will be detected in a high-resolution Muon Spectrometer with standalone triggering and momentum measurement. Muons with an energy of more than a few GeV penetrate the calorimeter and reach the Muon Spectrometer, which consists of drift-tubes chambers.

The correct alignment of the ATLAS Muon Spectrometer is crucial to ensure its design performance. This note documents the attempt of using various misaligned Muon Spectrometer layouts to study their impacts Muon Spectrometer performance. These impact on have been studied with a 50 GeV muon sample and a $Z \rightarrow \mu\mu$ sample. The samples have been simulated with an ideal Muon Spectrometer layout, while during reconstruction a misaligned layout has been assumend. An average uncertainty of roughly 1 mm in the chamber position deteriorates the momentum resolution from 4% to 9% for muons with a momentum of 50 GeV.

[1] present affiliation is Univ. Illinois at Urbana-Champaign, Department of Physics, USA
[2] Corresponding Author

1 Introduction

The ATLAS Muon Spectrometer [1], [2] provides three-point measurements of tracks in the field of large superconducting air-core toroid magnets. Its momentum measurement capability combines the highest possible efficiency with a momentum resolution of 2-3% at 10-100 GeV/c and 10% at 1 TeV (taking into account the high background environment, the inhomogeneous magnetic field, and the large size of the apparatus of 24 m diameter by 44 m length). In order to achieve the required precision of 10% in the momentum measurement, the sagitta must be determined with a precision of 50 μm over most of the pseudorapidity range. Precision measurement of the track coordinates in the principal bending direction of the magnetic field is provided by Monitored Drift Tubes (MDTs) and Cathode Strip Chambers (CSCs). The MDT chambers are arranged in three layers all around the calorimeter in order to determine the momentum with the best possible resolution. An optical alignment system controls the relative positioning of muon chambers at the 30 micron level. The CSCs are used for the very forward area where the particle flux is too high for the drift chambers.

With this layout, a three-point measurement is available (see FIG. 1) by installing three stations of MDT chambers covering the full rapidity range with high hermeticity.

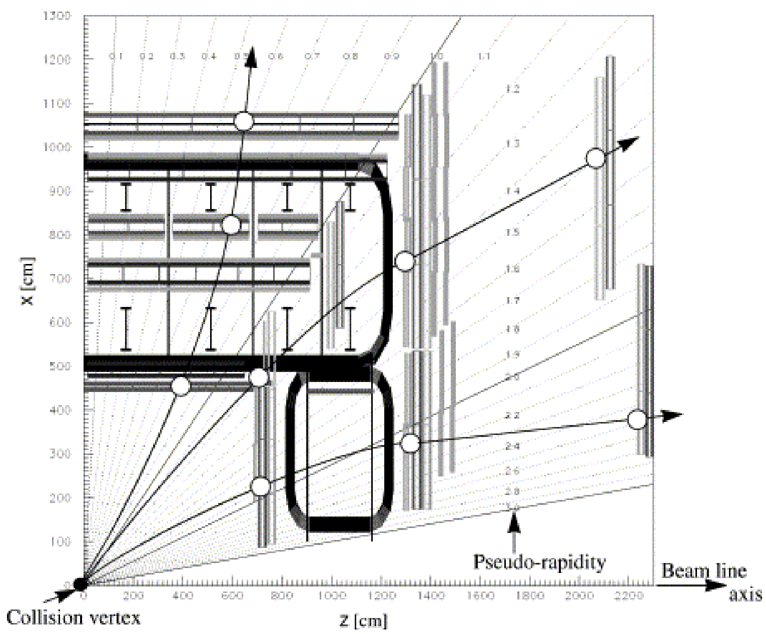

Figure 1: Longitudinal cross-section in the bending plane of the spectrometer showing the barrel and end-cap magnet air-coil toroid configuration. It shows the pseudo-rapidity coverage of the Muon Spectrometer from 0 to 2.8 and a sketch of the layout principle of the three detecting muon stations. Trajectories are shown for positively and negatively charged particles of a few GeV/c.

To achieve the benchmark resolution by a three-point measurement, with the size and bending power of the ATLAS toroids, each point must be measured with an accuracy of about 50 μm. This sets the scale for the requirements on the intrinsic resolution, the mechanical precision, and the survey accuracy of the muon chambers.

The momentum resolution of the spectrometer is limited by the intrinsic detector resolution, MDT calibration errors, chamber positioning uncertainties, multiple scattering, and statistical fluctuations of energy loss. At smaller momenta (below about 300 GeV), the resolution is limited by multiple scattering to a few percent, at higher momenta (above 300 GeV) it is dominated by chamber precision and alignment.

The design performance of the ATLAS Muon Spectrometer can be only achieved with a precise alignment of the chambers. The impact on the Muon Spectrometer performance of various misaligned layouts has been studied in this note. The note is structured as follows: In section 2 the studied quantities are introduced and the performance for an ideal Muon Spectrometer is discussed. Section 3 is dedicated to the implementation, validation and impacts of random misalignments on single muons as well as on $Z \rightarrow \mu\mu$ decays. Section 4 presents the validation of the so-called 'egg-shape' layout. The note closes with a short overview of possible alignment strategies and presents an alignment-method based on the decay of Z bosons into muons.

The following study is mainly based on a 10K single muon sample with a transverse momentum of 50 GeV, simulated and reconstructed within Athena-Release 12.0.6. The transverse momentum of 50 GeV was chosen because the Muon Spectrometer is expected to have its best performance at this energy. Moreover, standard physics processes like the decay of the W or Z boson, which play an important role in the first phase of LHC, have final state muons with this energy. An exception is section 4, which is based on a single muon sample simulated and reconstructed with Athena 10.0.4. An overview of all used samples can be seen in Table 1.

Sample	Software Version	Sample Size
Single Muons (50 GeV)	12.0.6	10,000
Single Muons (100 GeV)	12.0.6	1,000
Single Muons (50 GeV)	10.0.4	5,000
$Z \rightarrow \mu\mu$	12.0.6	5,000

Table 1: Overview of Monte Carlo samples used for this study

2 Overview of Ideal Muon Spectrometer Performance

The ATLAS Muon Reconstruction programs starts from *bytestream* data[1)], and converts the information into *reconstruction hits*. In the case of simulation the bytestream is simply a converted form of the digits. The reconstruction then performs pattern recognition and track fitting, taking into account the magnetic field and correcting for the energy loss in the calorimeter. A schematic sketch of the different components, leading to a reconstructed track, is shown in FIG. 2. A detailed description can be found in [3], [4].

The quantities *efficiency* and *resolution* are used for the validation and performance evaluation of the muon track reconstruction algorithms. Efficiency ε is defined as

$$\varepsilon := \frac{N_{\text{Correct Reconstructed Track}}}{N_{\text{Monte Carlo Truth Muons}}} \tag{1}$$

where a track is defined as correctly reconstructed if its transverse momentum p_T and its coordinates η and ϕ[2)] fulfill the condition

$$d_{\eta\phi} = \sqrt{\omega_1 \cdot (\eta - \eta^{Truth})^2 + \omega_2 \cdot (\phi - \phi^{Truth})^2 + \omega_3 \cdot \left(\frac{1}{p_T^{Truth}} - \frac{1}{p_T}\right)^2} \leq r_c. \tag{2}$$

[1)]Events in a format that is equivalent to coming directly from the read out electronics of the experiment.

[2)]The pseudo-rapidity η and the azimuthal angle ϕ are defined at the interaction point

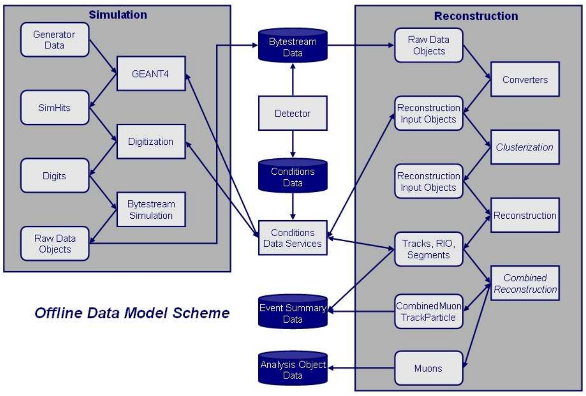

Figure 2: Schematic illustration of the Event Data Model.

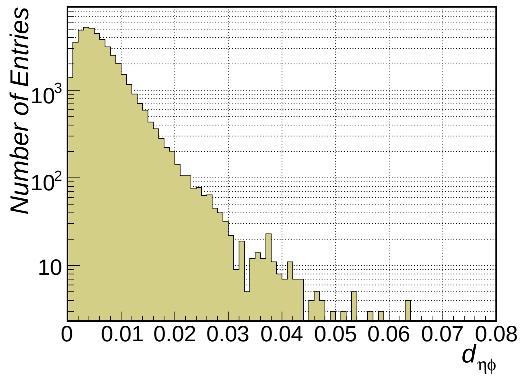

Figure 3: Distribution of the distance $d_{\eta,\phi}$ for 50 GeV single muon Monte Carlo Sample.

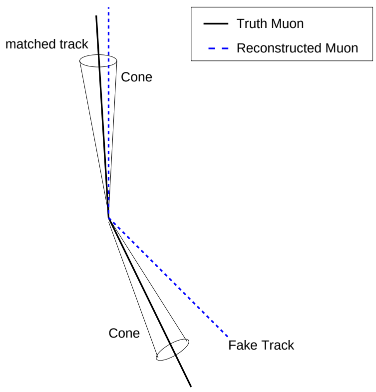

Figure 4: Illustration of matching two tracks.

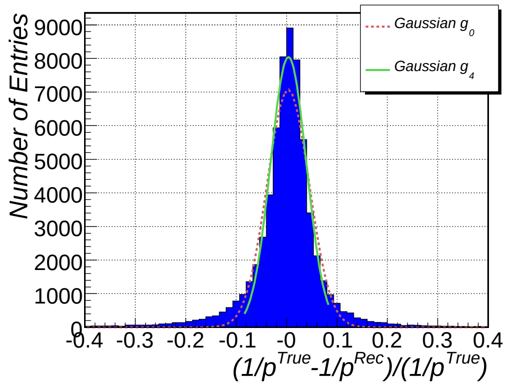

Figure 5: Definition of the transverse momentum (p_T) resolution. g_0 is the fitted Gaussian of iteration step 0, g_4 is the fitted Gaussian of iteration step 4.

Here, ω_1, ω_2 and ω_3 are weights for the three variables (η, ϕ, p_T) and r_c is the threshold value. Because misalignment is expected to have a significant effect on the p_T-resolution, and because setting $\omega_3 \neq 0$ would indirectly impact the reconstruction efficiency, it was chosen to set $\omega_3 = 0$. The weights for η and ϕ were set to $\omega_1 = \omega_2 = 1$.

FIG. 3 shows the distances, as defined by Equation 2, between generated and reconstructed muon tracks in a 50 GeV single muon sample. We require that the reconstructed transverse momentum does not differ by more than 10% from the corresponding truth value. A threshold value of $r_c = 0.05$ ensures that almost all reconstructed tracks can be matched to the corresponding truth tracks. By Equation 2, this condition requires that the reconstructed particle track lies within a cone of radius 0.05 around the truth muon track (FIG. 4).

Another important variable for Muon Spectometer performance is the transverse momentum (p_T) resolution. The normalized p_T deviation ρ for each correctly identified track is given by

$$\rho := \frac{\frac{1}{p_T^{Truth}} - \frac{1}{p_T^{Reconstructed}}}{\frac{1}{p_T^{Truth}}} = 1 - \frac{p_T^{Truth}}{p_T^{Reconstructed}} \tag{3}$$

and is plotted in FIG. 5. Note that we expect a Gaussian distribution for $\frac{1}{p_T}$, but not for p_T itself. Momentum measurement derives from the inverse of sagitta s measurement ($p \sim \frac{1}{s}$), which is subject to gaussian uncertainties. The p_T-resolution itself is defined in several steps. First, a Gaussian g_0 is fitted to the distribution. Next a second Gaussian g_i is fitted to the data between the $x_{m,i-1} \pm 2 \cdot \sigma_{g_{i-1}}$, where $\sigma_{g_{i-1}}$ is the width of g_{i_1} and $x_{m,i-1}$ its mean. Finally, this iterative procedure is repeated n times. It turns out that $n = 2$ steps are already enough to find a stable fit. The width of g_2 is then defined as p_T resolution. The mean of g_2 is referred to as the *momentum-scale*, which is a measure for a systematic shift of measured muon momenta.

The reconstruction efficiency distribution versus η for standalone and combined reconstruction is shown in FIG. 7. *Standalone reconstruction* refers to a muon track reconstruction which is exclusively based on Muon Spectrometer information. For this study, it was chosen to use the reconstruction algorithm called *Muonboy* [5], [6]. Alternatively, information from the inner tracking detectors could be used to perform the combined reconstruction algorithm called *STACO* [7]. The efficiency for both reconstruction methods is expected to be roughly equivalent, with a slightly lower reconstruction efficiency for the combined reconstruction. The drop of efficiency at $\eta \approx 0$ is due to holes for service passages in this region. Some MDT-chambers, the so-called EE type, are missing[3)] in the η-region $1.1 < |\eta| < 1.3$. This η-region corresponds to the transition between the Muon Spectrometer's barrel and the endcap, and explains the drop of efficiency at $|\eta| \approx 1$.

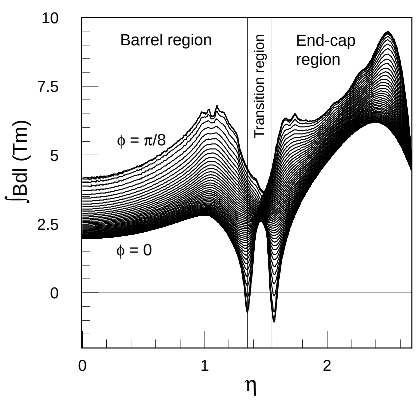

Figure 6: Bending power of the magnetic field in the ATLAS Muon Spectrometer vs. η.

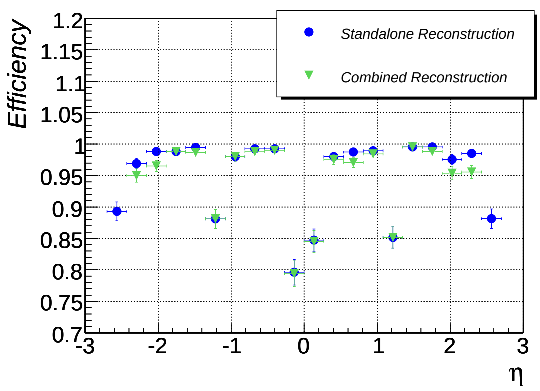

Figure 7: Muonboy Spectrometer reconstruction efficiencies for various reconstruction algorithms vs. η.

The p_T-resolution is roughly ϕ-symmetric, but has a relative strong η-dependence due to several design aspects of the Muon Spectrometer, as discussed in the following. Hence it is usually sufficient to study the η-dependence of the transverse momentum resolution. The p_T-resolution versus η is shown in FIG. 8. The resolution of the combined reconstruction is significantly better than the standalone reconstruction for the muon energy of 50 GeV. Large differences can be observed in the Barrel/Endcap transition region. Indeed in this region the absence of the EE type chambers imposes an angle-angle measurement which leads to a severe degradation of the momentum resolution. Moreover, the magnetic

[3)] These chambers are foreseen in the initial layout of the spectrometer, but their installationis staged.

field integral in this region is relatively weak, as illustrated in FIG. 6. The combined reconstruction resolution is driven by the Muon Spectrometer performance for $|\eta| > 2$. Note that the inner tracker covers an η-region from -2.5 to $+2.5$, while the Muon Spectrometer covers a region up to $|2.7|$.

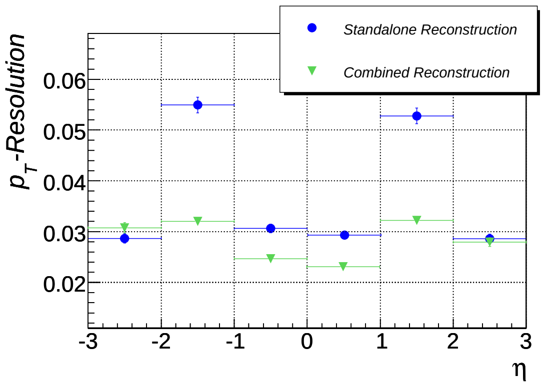

Figure 8: Muonboy p_T-resolution for various reconstruction algorithms vs. η.

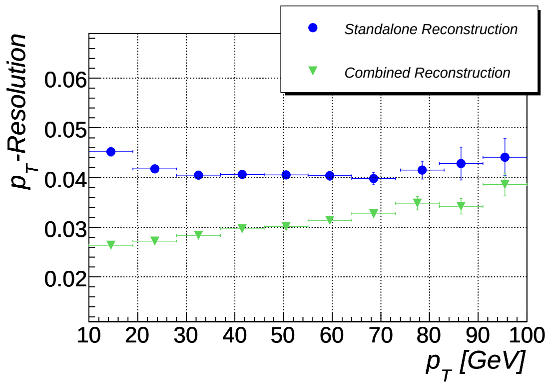

Figure 9: Muonboy p_T-resolution for various reconstruction algorithms vs. p_T of muons (based on a $Z \rightarrow \mu\mu$ sample).

The p_T-dependence of the resolution is shown in FIG. 9. While we observe a linear worsening of the combined reconstruction resolution, a more complicated behavior is seen for the standalone reconstruction. The resolution improves up to an energy of roughly 50 GeV, then it worsens with increasing p_T. This can be explained by the different effects which impact the p_T-resolution: Multiple scattering effects are independent from the p_T itself and are dominating the resolution at around 100 GeV. For low p_T muons, enery loss in the calorimeter is the dominating contribution to, roughly 3% at 10 GeV but only 0.5% at 100 GeV. Conversely, the contribution of the intrinsic resolution of the precision chambers and their alignment is small at low momenta. However, above a p_T of around 100 GeV it starts to rise and quickly dominates. For muons with p_T roughly above 100 GeV, the spectrometer provides a better resolution than the inner detector and becomes the dominant component for combined reconstruction.

3 Random Misalignment

3.1 Implementation

The alignment of Muon Spectrometer chambers will be a long and challenging task. It is thus worth investigating the impact on performance of imperfect knowledge of geometry.

The position of each chamber can be described by 6 parameters, three position parameters in space and three defining the rotations. Each position and angle is expected to be displaced from its nominal value by a certain amount. In order to model these displacements we introduce a dimensionless variable called the *misalignment parameter* σ_m^{All}. The value of this parameter corresponds to the width of a Gaussian function which is centered around zero. Position parameters and rotation angles of all MDT-chambers is smeared independently by this Gaussian, multiplied by $1\,mm$ in the case of translations or $1\ mrad$ in the case of rotations[4)]. We have chosen one standard misaligned Muon Spectrometer layout, which was generated with $\sigma_m^{All} = 1$ (i.e. all chambers are randomly shifted by a mean of 1 mm and are rotated by a mean of 1 *mrad*). New survey measurements at the Endcap-region of the Muon Spectrometer have shown that these misaligments, assumed during reconstruction, are of the right order of magnitude, but might be underestimated to a certain degree [5)].

Note that an MDT-chamber can also be internally misaligned, i.e. the two multi-layers can be rotated and shifted with respect to each other and even the layers within the multilayers might be affected by distortions [8]. This aspect of misalignment has not been studied here. Nevertheless, tomograph measurements have shown that these internal misalignments do not exceed $30\,\mu m$.

In order to describe the misplacements and rotations in a common way for all chambers, a new coordinate system is defined for each MDT-chamber separately, which is illustrated in FIG. 10. The s-axis is defined as the tube direction, the z-axis in the plane defined by one multilayer and perpendicular to the s-axis. The t-axis is defined to be perpendicular to the other two axis. The corresponding rotations are also illustrated in FIG. 10. Rotation around the s-axis is defined by the angle γ and is applied on one end of the MDT-chamber. The corresponding rotations around the z-axis and t-axis are defined by the angles β and α, respectively.

The most important aspect of misalignment is the difference in performance of a perfectly aligned layout and an uncorrected misaligned one. In other words, to what precision must the Muon Spectrometer be aligned, to achieve a certain performance?

In answering this question, the principle is to have different descriptions of the geometry at simulation and at reconstruction levels. Hereafter the simulation description will be called 'simulation layout' and the reconstruction description will be called 'reconstruction layout'. In order to study these differences in principle one has to use a misaligned layout during the simulation step and an ideal or a misaligned layout during reconstruction.

The Geant4 simulation and the corresponding digitization of events requires an intensive computational calculation, while the reconstruction of such an event from the simulated digitized data is orders of magnitude faster. In order to test the effects of several different misaligned Muon Spectrometer layouts it is very helpful to test the equivalence of the misalignment impacts on the Muon Spectrometer performance for the following two cases:

- Case 1: using a misaligned 'simulation layout' and an ideal 'reconstruction layout'.
- Case 2: using an ideal 'simulation layout' and a misaligned 'reconstruction layout'.

[4)] Note that these rotations are not applied in the center of one MDT-chamber but at the middle of one of its edges.

[5)] Translations and rotations of the nominal positions of MDT-chambers in the order of $2-4$ mm and $2-4$ *mrad* have been measured

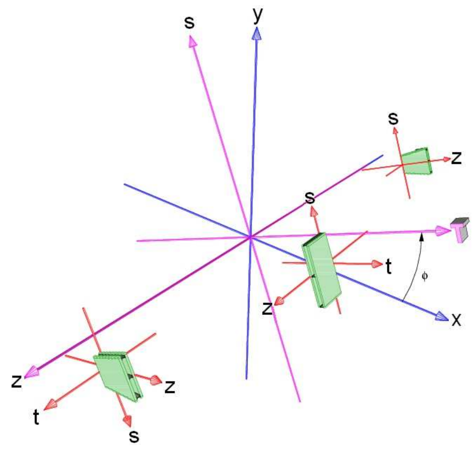

Figure 10: Illustration of Misaligned Chambers.

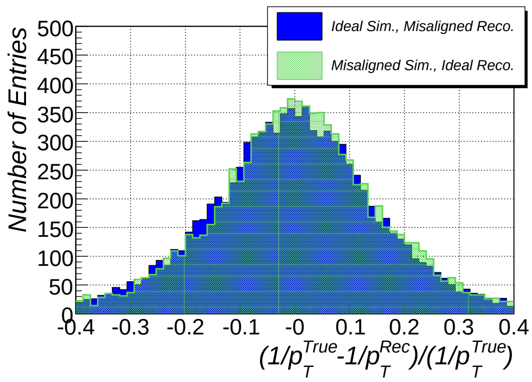

Figure 11: Comparison of two p_T-resolution distributions for a 50 GeV single muon sample, simulated with nominal layout and reconstructed with misaligned layout and vice versa.

FIG. 11 shows, for both cases, the overall comparison of the p_T-resolution distribution for a 50 GeV single muon sample. FIG. 12 and 13 show the corresponding p_T-resolution and reconstruction efficiency comparison, respectively. No significant differences can be observed for the reconstruction efficiency, but a slightly better p_T-resolution for case 1 (FIG. 12). The same η-dependence of the resolution can be observed for both cases. The relative difference of the p_T-resolution is about 2.5%, which must be treated as a systematic uncertainty if one draws conclusions from case 1 to case 2 or the other way round. Several effects can cause this relatively small difference. One possibility is the difference in the magnetic field which is assumed during the simulation and the reconstruction, since the muons interact with the gas in the tubes at different positions for the two layouts. Hence a different effect on positive and negative muons is expected.

Moreover a small difference between case 1 and 2 in the momentum scale can be observed, which is 0.006 ± 0.002. This is explained in detail in the following.

First of all it must be noted that case 1 and 2 are not equivalent on an event-by-event basis. Comparing the reconstruction of muons for both cases, where the muons are based on the same truth information (η, ϕ and p_T), will reveal differences in the reconstructed muon track for each event. This can be easily understood, since shifts of a misaligned layout will lead to opposite effects if they are used during simulation or during reconstruction. This effect is illustrated in FIG. 14 and FIG. 15.

The effect can be studied, by comparing positive and negative muons separately. The effect on the reconstructed momentum scale versus η is shown separately for positive and negative muons in FIG. 16. Note, that each η bin averages over 16 chambers in ϕ-direction and over two or more sectors in the η-direction, hence a net-shift is expected. A net-shift Δs on the sagitta s leads to a shift of the reconstructed transverse momenta:

$$p_T^{\mu_+} \sim \frac{1}{s + \Delta s}, \qquad\qquad p_T^{\mu_-} \sim \frac{1}{s - \Delta s}.$$

The momentum scale for a given η-bin and a specified muon charge is not expected to be null. Moreover, the momentum scale shift for a given muon charge will differ only by the sign of the charge. The momentum scale shift will reverse with the muon charge sign. It is expected that the momentum scale shifts will be opposite for positive and negative muons. As seen by comparing the two plots of FIG. 16, this is true up to statistical fluctuations.

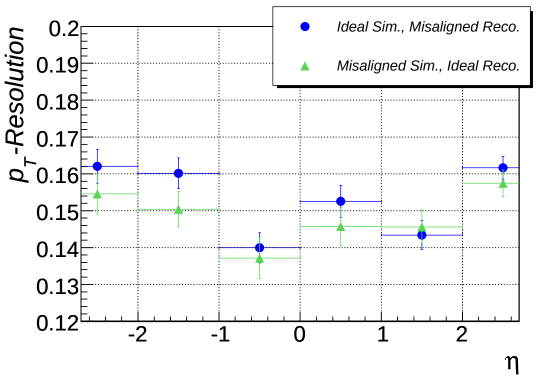

Figure 12: Comparison of two p_T-resolution distributions for a 50 GeV single muon sample, simulated with nominal layout and reconstructed with misaligned layout and vice versa vs. η.

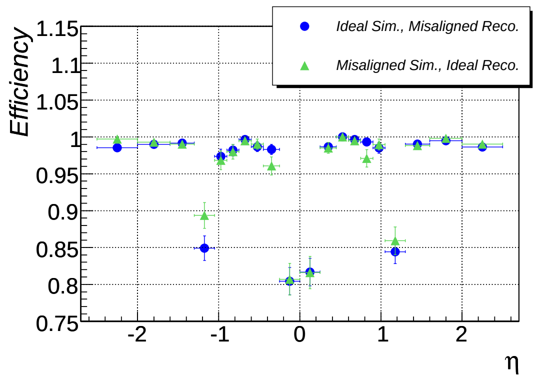

Figure 13: Comparison of reconstruction efficiency for a 50 GeV single muon sample, simulated with nominal layout and reconstructed with misaligned layout and vice versa.

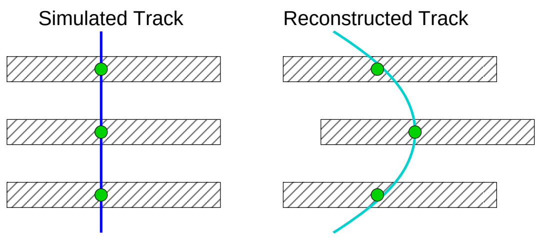

Figure 14: Illustration of the impact on reconstructed tracks using an ideal *simulation layout* and a misaligned *reconstruction layout*.

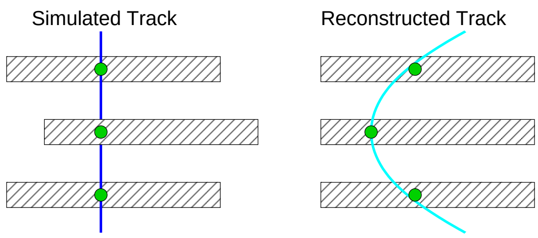

Figure 15: Illustration of the impact on reconstructed tracks using a misaligned *simulation layout* and a ideal *reconstruction layout*.

The other aspect is to study the equivalence of using an ideal layout during the simulation and the reconstruction step, and a misaligned layout during simulation but a corrected (i.e. perfectly aligned) layout during reconstruction. The latter case is nothing more than using the same misaligned layout for reconstruction that it is used for simulation. An equivalence is a strong hint that the alignment of the Muon Spectrometer leads to the expected design performance. The position of each MDT-chamber in space is not too relevant so long as the position is known to a high accuracy. FIG. 17 illustrates the comparison of the overall p_T-resolution and FIG. 18 the p_T-resolution in both cases. Both results coincide within their statistical uncertainties.

The comparison of muon reconstruction efficiency vs. η is shown in FIG. 19. Again, no significant difference can be observed within our statistics. Note that some features of a non ideal layout induce degradation of performance, even if the geometry is perfectly known. For example, this is the case with non-parallelism of tube station to station. If for instance, the outer and inner tubes are parallel but the middle tubes are not parallel with respect to the other two stations, then the precison on the 2nd coordinate will enter in the precision of the position measured in the bending plane, ideally given by the middle tubes precision only. Even if the non parallelism is prefectly known, this cannot be recovered. The available statistics were too small to observe these minor effects.

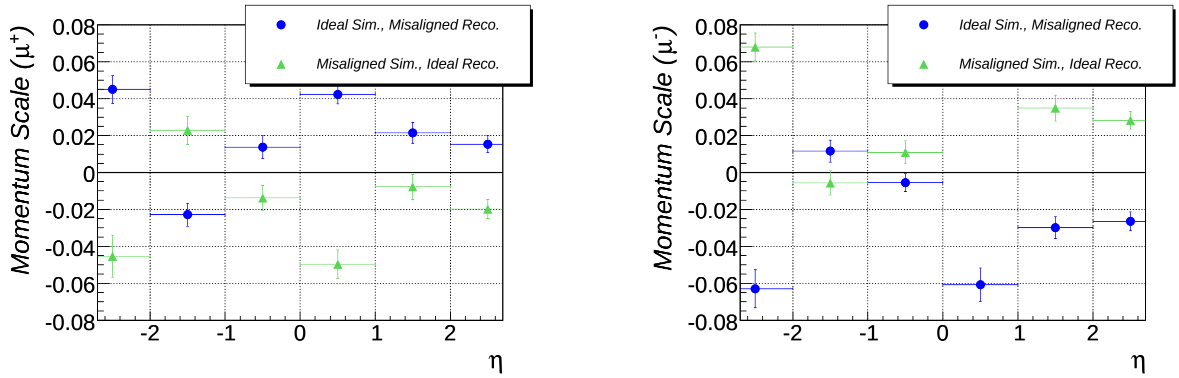

Figure 16: Comparison of the momentum scale for 50 GeV same charged muons simulated with ideal layout and reconstructed with misaligned layout and vice versa: μ^+ left, μ^- right

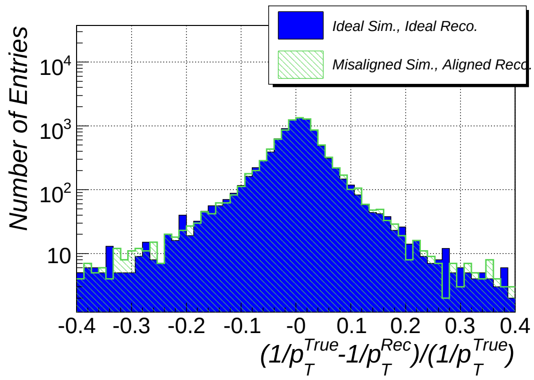

Figure 17: Comparison of p_T-resolution distribution for an aligned nominal layout and an aligned distorted layout.

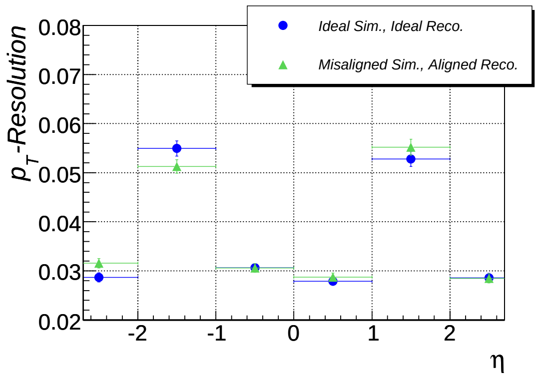

Figure 18: Comparison of p_T-resolution vs. η for an aligned nominal layout and an aligned distorted layout.

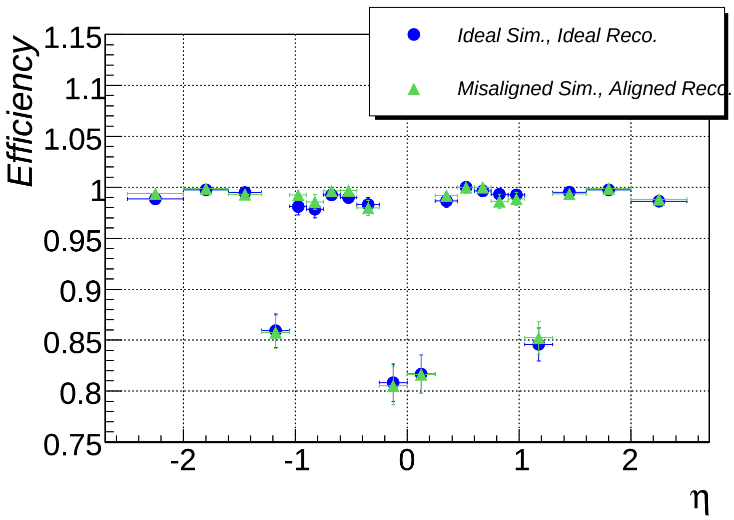

Figure 19: Comparison of reconstruction efficiency vs. η for an aligned nominal layout and an aligned distorted layout, respectively.

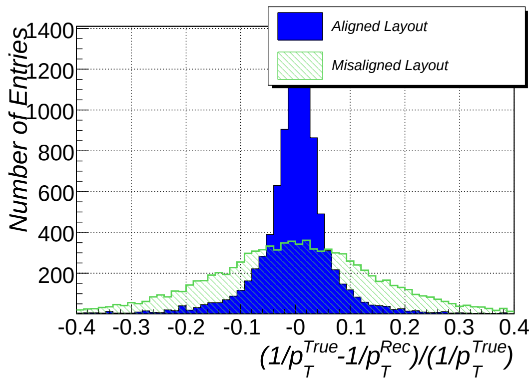

Figure 20: Comparison of p_T-resolution distribution for an aligned Muon Spectrometer and a misalingned Muon Spectrometer with $\sigma_m^{All} = 1$.

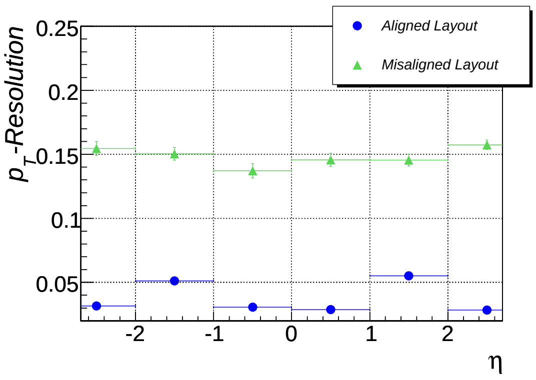

Figure 21: Comparison of p_T-resolution for an aligned Muon Spectrometer and a misaligned Muon Spectrometer with $\sigma_m^{All} = 1$.

3.2 Misalignment in all six parameters

To study the effect of an uncorrected misaligned layout on the reconstruction performance, the standard misaligned layout was used during the reconstruction phase of a sample. This layout corresponds to a misaligned parameter $\sigma_m^{All} = 1$, using a sample simulated with an ideal layout. FIG. 20 shows the comparison of the p_T-resolution for an aligned and a misaligned Muon Spectrometer. As expected, a large broadening of the p_T-resolution distribution can be observed in the case of misalignment. A graph of p_T-resolution vs. η is illustrated in FIG. 21The misalignment impact dominates the overall resolution.

The overall observed resolution σ_{All} can be expressed as the quadratic sum of the p_T-resolution of the ideal geometry (σ_{ideal}) and the resolution due to the misaligned geometry ($\sigma_{Alignment}$).

$$\sigma_m^{All} = \sqrt{\sigma_{Alignment}^2 + \sigma_{ideal}^2}$$

This leads to $\sigma_{Alignment} \approx 0.14$ for muons with $p_T \approx 50\,\text{GeV}$.

A misaligned layout leads to no significant decrease in the reconstruction efficiency as illustrated in FIG. 22. This result has the consequence that a heavily misaligned Muon Spectrometer can stil be used for muon identification of inner tracks during the very first phase of the experiment, without applying any corrections and assuming no further information from the optical alignment sensors. Nevertheless, only a highly precise aligned Muon Spectrometer provides the design momentum resolution.

We expect a flat p_T-resolution for muons with transverse momenta between 10 GeV and 100 GeV. As already discussed in section 3.1, the p_T-resolution in this momentum range is dominated by multiple scattering effects and possibly, by misalignment. The behavior of p_T-resolution to increasing p_T reveals a strong linear correlation, which is illustrated in FIG. 23[6]. This linear worsening of the resolution can be explained by the inverse dependence of the measured sagitta s and the corresponding momentum, $s \sim \frac{1}{p}$. It follows, that

$$p \cdot \Delta s \sim \frac{\Delta p}{p}, \tag{4}$$

The uncertainty in the measured sagitta has several contributions, e.g. multiple scattering effects, which scale as $1/p$. However, the impact of relatively large misalignments, considered here, dominates

[6] The measured points of the misaligned layout have not been corrected for the p_T-distribution of muons resulting from a Z boson decay. An exception is the point at 100 GeV which was determined with a 100 GeV single muon sample.

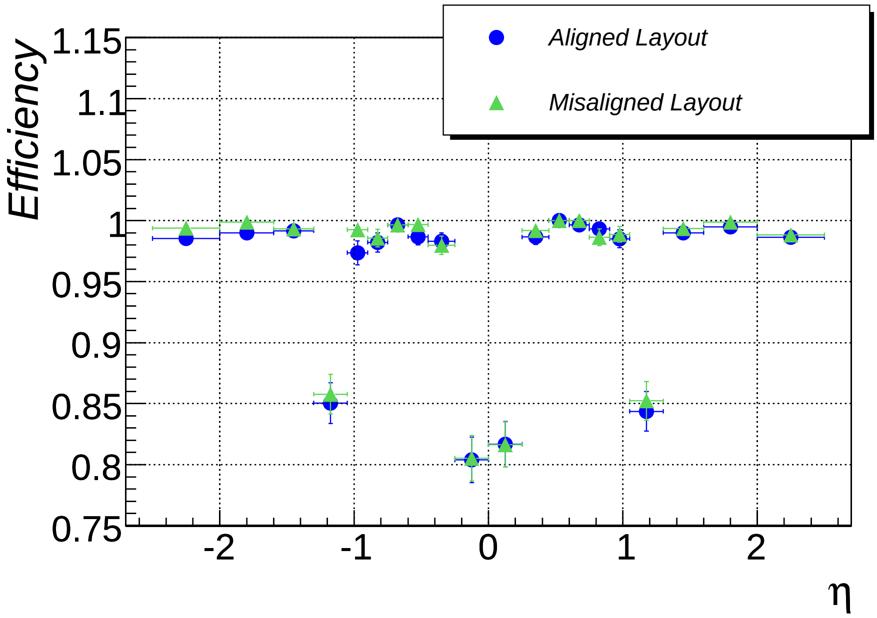

Figure 22: Comparison of reconstruction efficiency for an aligned Muon Spectrometer and a misalingned Muon Spectrometer with $\sigma_m^{All} = 1mm$.

the overall uncertainty of sagitta. Hence it can be assumed that Δs is approximately independent of the track momentum, even for small momenta.

Layouts with various values of the misalignment parameter σ_m^{All} have been used for the muon reconstruction. The p_T-resolution increases with increasing misalignment parameter (see FIG. 24). The behavior can be parameterized by the function:

$$\sigma_{res} = \sqrt{\sigma_{ideal}^2 + a \cdot (\sigma_m^{All})^2} \tag{5}$$

where σ_{ideal}^2 corresponds to the resolution if no misalignment is present. Fitting Equation 5 to the measured resolution vs. the misalignment parameter in FIG. 24 leads to $a \approx 0.021$ and $\sigma_{ideal} \approx 0.037$. Hence, a misalignment parameter of 0.05 leads only to a relative increase by 2% of the p_T-resolution for 50 GeV muons, which is effectively negligible and in very good agreement to the alignment goal of the Muon Spectrometer.

3.3 Misalignment impacts on the Z boson resonance

The impact of a misaligned Muon Spectrometer layout ($\sigma_m^{All} = 1$) on the reconstructed Z boson mass is shown in FIG. 25. Since the momentum scale of the reconstructed muon p_T is very little affected by misalignment, it is expected that the mean of the invariant mass distribution does not change significantly. On the other hand a large broadening of the distribution due to the worsening of the p_T-resolution of the muons is expected.

The reconstructed di-muon mass distribution f_Z^{Reco} can be described by the convolution of the Monte Carlo predicted mass distribution f_Z^{MC} with a Gaussian function,

$$f_Z^{Reco} = \int A \cdot f_Z^{MC}(m_Z, \Gamma_Z) \cdot e^{-\frac{(x_m - m_Z)^2}{2 \cdot \sigma_g^2}} \cdot dm_Z$$

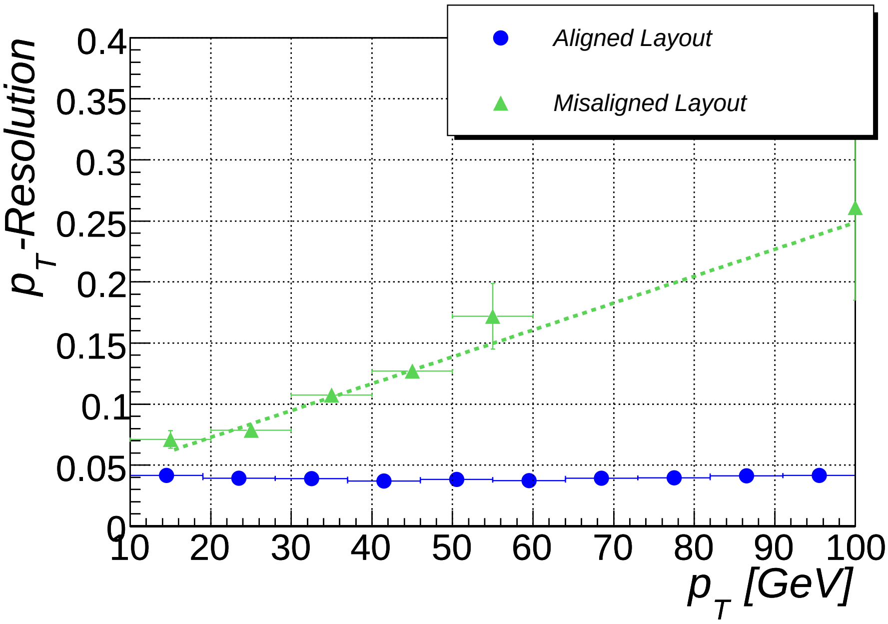

Figure 23: Comparison of p_T-resolution width for an aligned Muon Spectrometer and a misalingned Muon Spectrometer with $\sigma_m^{All} = 1mm$(based on a $Z \to \mu\mu$ sample). The p_T-resolution for the aligned layout was shown in more detail in Figure 9

where A is a global normalization factor, x_m the mean-mass and σ_g the width of the Gaussian. The PYTHIA prediction of the Z boson mass distribution is described by the function f_Z^{MC}. A simple Breit-Wigner function for f_Z^{MC} is not used, since this would not reflect the Z/γ^*-mixing for lower invariant masses.

The dependence of x_m and σ_g on the misalignment parameter is shown in FIG. 26 and FIG. 27, respectively. A linear dependence for the measured width of the reconstructed Z boson mass distribution can be observed for misalignment parameters above 0.2. No systematic effect on the mean of the reconstructed Z boson mass is seen[7)].

3.4 Shifts in special-directions

So far only misalignment parameters have been studied which affect both translations and rotations. In this section, the effect of translations and rotations of MDT-chambers is studied independently. FIG. 28 shows p_T-resolution versus η for misaligned layouts based on misalignment parameters $\sigma_m^{s,t,z} = 1$. It is expected that misalignment along the z-axis has a dominant effect, since this translation directly affects the sagitta measurement. Misalignment along the s-axis should have no effect on the p_T-measurement, since it corresponds to a translation along the drift-tubes. Also, misalignment along the t-axis of each chamber is expected to have only a very limited contribution to the p_T-resolution since this translation is almost parallel to the muon trajectory. This can be seen in FIG. 28, which demonstrates the validity of these predictions.

The impact on the p_T-resolution of $\sigma_m^{Rot} = 1$, where only random rotations are applied, is shown in

[7)] To a first approximation, misalignment effects are symmetric for positive and negative muons and therefore largely cancel each other.

FIG. 29. Note a significantly larger effect due to rotations compared to translations on the p_T-resolution. This can be explained by the definition of the misalignment parameter and the application of rotations. The rotation of one MDT-chamber with a length of 6 *m* by 1 *mrad* leads to difference in the position of 6 mm for the tube ends. This relative shift of 6 mm is dominant compared to a translation of 1 mm, both induced by a misalignment parameter $\sigma_m^{All} = 1$.

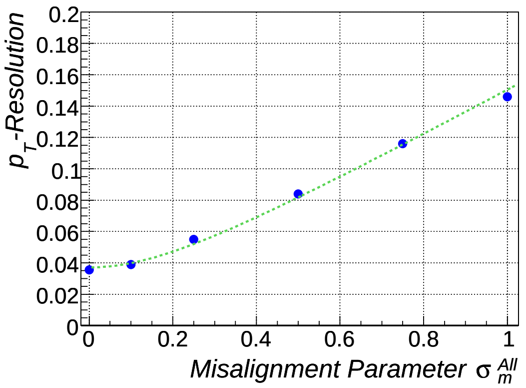

Figure 24: p_T-resolution vs. misalignment parameters σ_m^{All} for a 50 GeV muon sample.

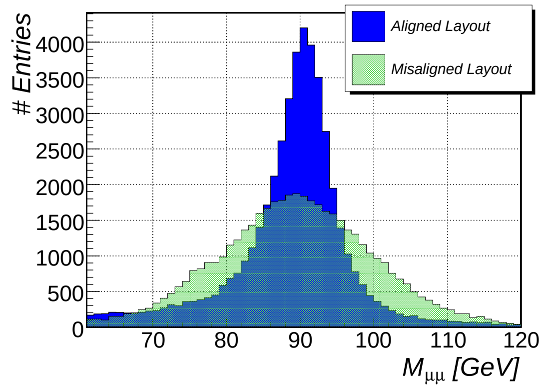

Figure 25: Reconstructed invariant di-muon mass distributions for an aligned and misaligned ($\sigma_m^{All} = 1$) layout.

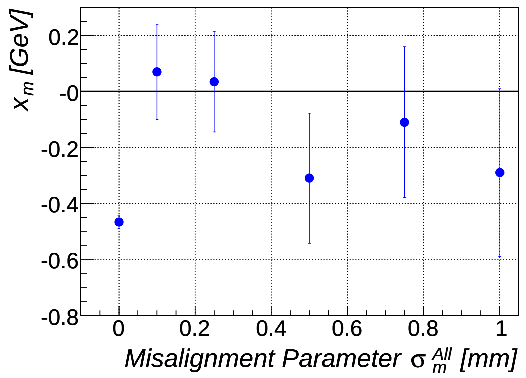

Figure 26: Mean of Gaussian x_m vs. misalignment parameter σ_m^{All}.

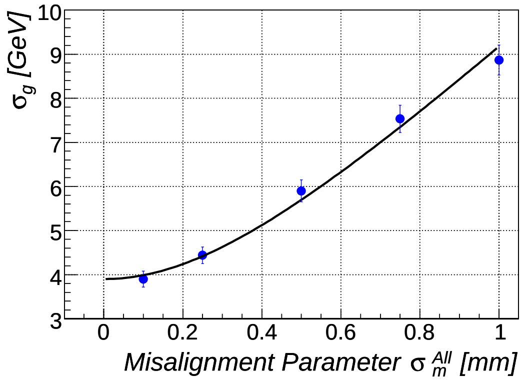

Figure 27: Width of smearing Gaussian σ_g vs. misalignment parameter σ_m^{All}.

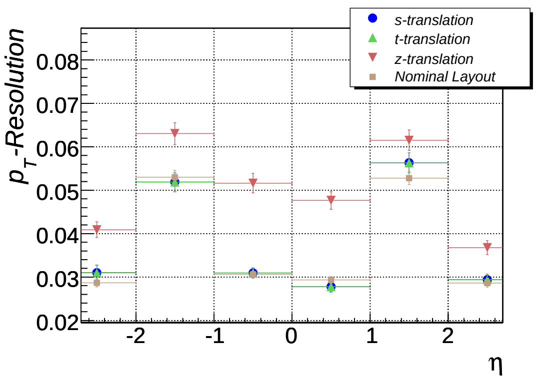

Figure 28: p_T-resolution distribution for independent translations.

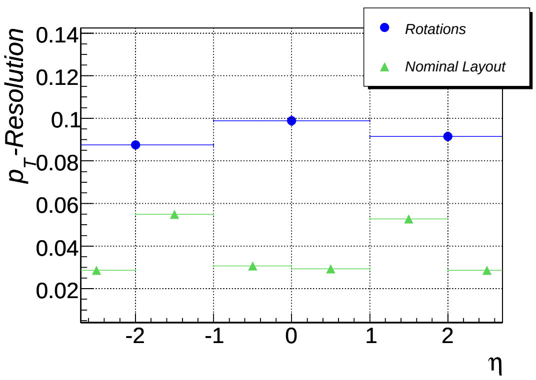

Figure 29: p_T-resolution distribution for independent rotations.

4 Egg shape Layout validation

During the life-time of the experiment, deformations of the ATLAS detector are expected due to its own weight of roughly 7.000 tons. To account for these deformations and to have perfect circular symmetry after the first years of operation, it was decided to build the Muon Spectrometer not with perfect circular symmetry, but with a small 'egg-shape' deviation. This is schematically illustrated in FIG. 30. This layout was implemented in the geometry description of the Muon Spectrometer. The chambers in sector 5 are systematically shifted by 7 mm in y-direction, the chambers in sector 1 and 9 are shifted by 3.5*mm* in x- and y-direction in the global coordinate system. The MDT-chambers in sector 13 as well as the endcap-region of the spectrometer are not affected by the egg-shape layout. All other chambers were rotated and shifted to be tangent to the assumed 'egg-shape' of the layout. Hence, the 'egg-shape' layout introduced a ϕ-asymmetry in the Muon Spectrometer geometry[8)].

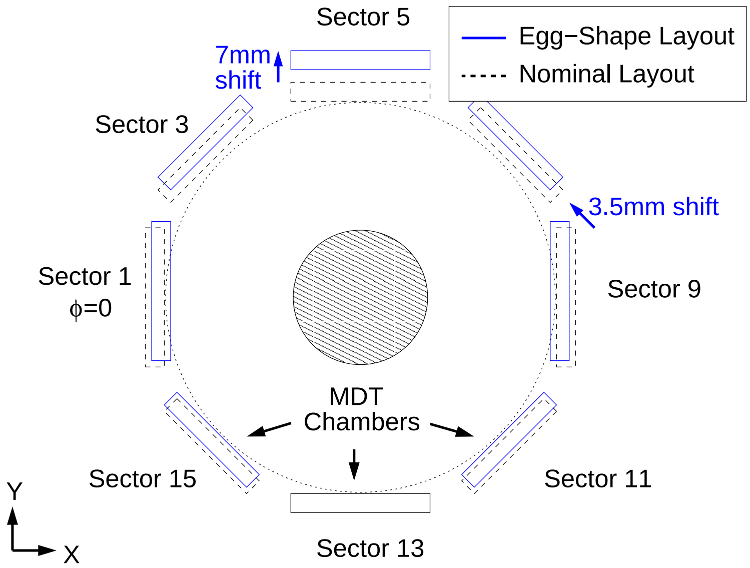

Figure 30: Schematic illustration of the 'egg-shape' layout.

It was chosen to use the 'egg-shape' layout during the reconstruction step, when the simulation was based on the ideal symmetric layout. No effects on the p_T-resolution, or as on the reconstruction efficiency, could be observed within the available Monte Carlo statistics. This is expected since the relevant displacements of the chambers are along axes which have only a weak effect on a possible shift of sagitta, as shown in section 3.4. Nevertheless, a detailed study of the 'egg-shape' layout offered the possibility to validate the standalone reconstruction algorithms based on minor changes in the geometry description.

As previously mentioned, the impact of the 'egg-shape' layout on the p_T-resolution is very small. The p_T-resolution of the ideal aligned Muon Spectrometer already dominates and therefore covering the expected effects. Hence it was chosen to compare muon tracks reconstructed with an ideal spectrometer layout and the 'egg-shape' layout on an event by event basis. In other words, the reconstructed track within one layout was directly compared to the reconstructed track of the same simulated muon within another layout.

The difference in the reconstructed transverse momenta for both layouts should show a ϕ-dependence

8)Note, that the assumed shift of 7 mm in the simulated layout is overestimated. The actual shift in the Muon Spectrometer is only 4 *mm*.

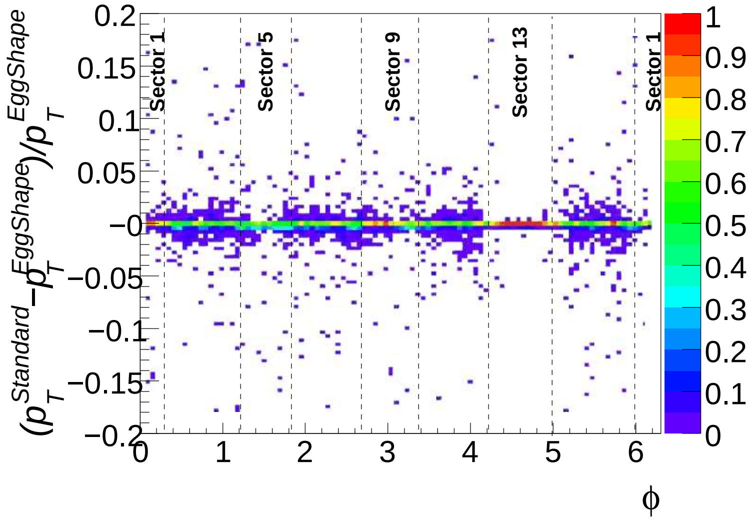

Figure 31: Difference in reconstructed p_T's with nominal layout and reconstructed p_T's with 'egg-shape' layout.

in the barrel region. No difference is expected for sector 13, and a relatively small impact in sectors 1, 5 and 9. FIG. 31 confirms this expectation.

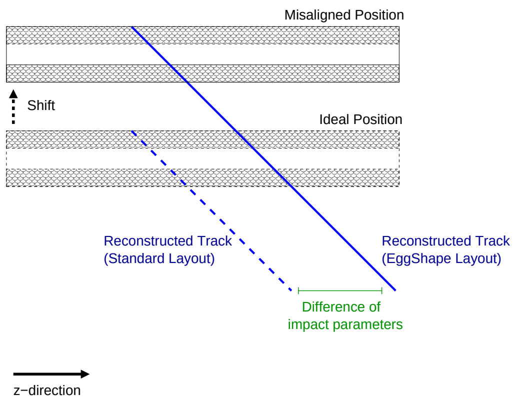

Figure 32: Schematic illustration of the 'egg-shape' effect on the longitudinal impact parameter z_0.

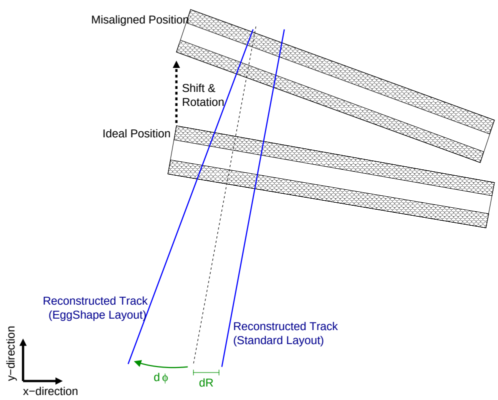

Figure 33: Schematic illustration of the 'egg-shape' effect on the transverse impact parameter d_0.

The longitudinal impact parameter z_0 describes the distance of closest approach to the interaction point of a reconstructed track where the interaction point is defined in the ATLAS coordinate system at (0,0,0). Note that a muon track, which has been reconstructed standalone by the Muon Spectrometer, must be extrapolated to the beam line. The longitudinal impact parameter z_0 is also effected by the 'egg-shape' layout. This can be most easily understood by considering an MDT-chamber in sector 5 next to the Endcap. The corresponding η-value of this chamber is 1, which corresponds to an angle of 40°. Assuming that muon tracks are straight lines, which is justified for 50 GeV muons, a shift of chambers in y-direction leads to an equivalent shift in the z-direction for tracks at beam level. This is illustrated in FIG. 32. No effect is expected for chambers at 0°. The average difference of the reconstructed impact parameters z_0 for both layouts of the muons, is shown in FIG. 34 and FIG. 35 for sector 1 and sector 5 respectively. As expected, a linear dependence is observed starting from $7mm$ in the case of sector 1 and from $3.5mm$ in the case of sector 5 to $-7mm$ and $-3.5mm$.

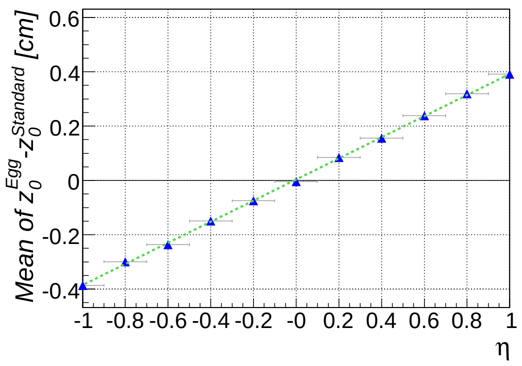

Figure 34: Difference of reconstructed impact parameter z_0 with nominal layout and with 'egg-shape' layout vs. η for Sector 1.

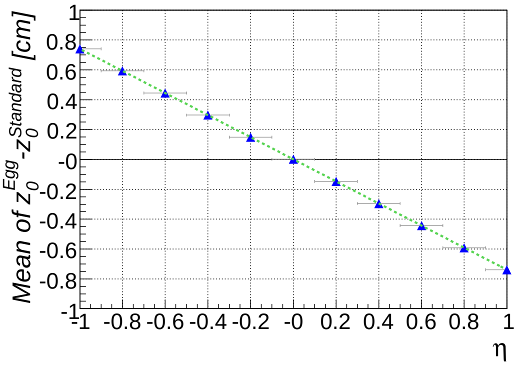

Figure 35: Difference of reconstructed impact parameter z_0 with nominal layout and with 'egg-shape' layout vs. η for Sector 5.

Introducing the quantity L_0, which is defined by

$$L_0 = d\phi \cdot d + dR_0 \tag{6}$$

allows a further validation, which is based on the ϕ measurement of the Muon Spectrometer. The quantity $d\phi$ is the difference of the measured ϕ-value comparing the reconstruction of a muon track for both layouts, dR_0 is the difference of the reconstructed transverse impact parameters d_0[9]. The distance d from the beam line to the outer barrel chamber is approximately 9800 mm. It is assumed that in the barrel region the ϕ-measurement is driven by the outer MDT- and RPC-chambers[10]. The quantity L_0 can be interpreted most easily for sector 1 and 9, where it reflects the chamber shift in the y-direction. The interpretation for sectors 3 and 7 is illustrated in FIG. 33, where it corresponds to the overall displacement of the chambers along the s-axis, defined in FIG. 10.

Sector	$d\phi$	dR_0 [mm]	Measured L_0 [mm]	Expecteed $L_0[mm]$
1	$(-2.7\pm0.3)\cdot10^{-4}$	-1.1 ± 0.1	-3.65 ± 0.3	-3.5
3	$(-3.0\pm0.3)\cdot10^{-4}$	-1.5 ± 0.2	-4.44 ± 0.4	-4.9
7	$(+2.8\pm0.3)\cdot10^{-4}$	1.7 ± 0.2	$+4.44\pm0.4$	+4.9
9	$(+2.5\pm0.3)\cdot10^{-4}$	1.4 ± 0.1	$+3.85\pm0.3$	+3.5

Table 2: Comparison of measured and expected values of L_0 for different sectors.

The measured average values for $d\phi$, dR_0 and the resulting L_0 - as well as the values, which are expected by geometrical considerations (FIG. 33) - are shown in Table 4 for four sectors. The measured and expected values of L_0 coincide within their statistical uncertainty. The presented validation tests can

[9] The impact parameter d_0 is defined by $\sqrt{x_0^2+y_0^2}$ and hence is the distance of the track to the line $x=y=0$

[10] It should be noted that the ϕ-reconstruction is exclusevily based on the Muon Spectrometer. Furthermore, we only consider the case, where the simulated samples are equivalent in both cases and only differ by the used geometry during reconstruction. Hence all uncertainties are highly correlated.

be considered as a first hint that the standalone reconstruction algorithms interpret even very sophisticated layouts like the ’egg-shape’ layout correctly.

5 Alignment and Determination of Sagitta-Shifts with the process $Z \to \mu\mu$

The general alignment-method of the Muon Spectrometer is the optical alignment system, which is expected to reach a relative precision between chambers within one tower up to 30 μm and an absolute precision in space of 300 μm for MDT chambers in the *large* sectors [2]. The precision for MDT chambers in the *small* sectors is less precise and therefore a track-based alignment between large and small chambers will be used [9].

Further methods for alignment have been proposed to allow independent cross-checks of the optical alignment method. One approach, studied in detail in [11], makes use of the measured deflection angle in the inner and outer stations to extrapolate the relative positions of the MDT-chambers. A relative alignment can be also achieved by measuring the p_T in each MDT-chamber separately, which was first proposed in [10], and used and studied also in [11].

The extrapolation of tracks, which have been reconstructed in the Inner Tracker, could lead to an absolute alignment of the Muon Spectrometer. In a first step, the extrapolated inner track would be compared to a corresponding measured segment in an inner MDT-station. This comparison will yield to alignment information regarding the MDT chamber. Having aligned all inner MDT stations, the extrapolation can be extended to the middle stations and in a final step to the outer stations. This procedure has the advantage that it allows an alignment relative to the Inner Tracker. The serious disadvantages are obvious. First the method relies on a perfectly aligned Inner Tracker. Secondly, the material description between the Inner Tracker and the Muon Spectrometer must be very precise in order to account correctly for multiple scattering and energy loss fluctuations mainly in the calorimeter.

The method presented here, is based on the decay of Z bosons into two muons. The goal is to determine the net-shift in sagitta for each MDT tower (i.e. three MDT-stations) but not to determine the exact positions of the MDT-chambers in space. Of course it has to be tested wether or not the assumption of an overall shift in sagitta is justified. FIG. 36 shows the p_T-resolution of positive muons for the three MDT-chambers in barrel A-2[11] and ϕ-sector 1, where the positions of the chambers were misaligned based on $\sigma_m^{All} = 1$. The p_T-resolution has slightly broadened. Even more importantly, however, a significant shift of the mean can be observed. Negative muons are expected to have a shift in the opposite direction by the same amount. This is a first hint that the p_T-resolution for each tower can be modeled in a first approximation by a shifted ideal p_T-resolution distribution. The broadening of the overall p_T-resolution can be therefore interpreted as the sum of several shifted ideal p_T-resolution distributions. Note that the net-sagitta Δs of each tower is directly correlated to the shift of the p_T-resolution, via

$$p_T \sim \frac{1}{\frac{1}{p_T} \pm \Delta s} \approx p_T(1 \mp p_T \Delta s) \tag{7}$$

The basic idea of the method is to make use of the correlation between the measured mean of the reconstructed Z boson mass distribution and the momentum scale of the muons. Note that the independence of the measured mean from the misalignment parameter, presented in FIG. 26, is due to averaging over the muon charges. An independent momentum scale $s_i^\pm$, which can be introduced for each tower i, changes the measured transverse momentum $p_{T,i}$ of each muon track, by

$$p_{T,i}^{scaled} = p_{T,i}(1 + s_i^\pm) \tag{8}$$

and increases or decreases the measured momentum. The value of $s_i^\pm$ might be chosen so that

$$s_i^\pm = c_\mu s_i \tag{9}$$

[11] This corresponds to an η-region of $0.2 < \eta < 0.45$

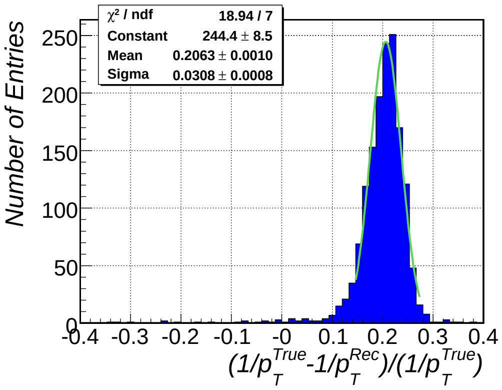

Figure 36: Transverse momentum resolution for a single misaligned MDT-tower (Barrel A-2, ϕ-sector 1) for 50 GeV positive muons. Note, that the resolution in the MDT-tower is better than the average resolution of the Muon Spectrometer.

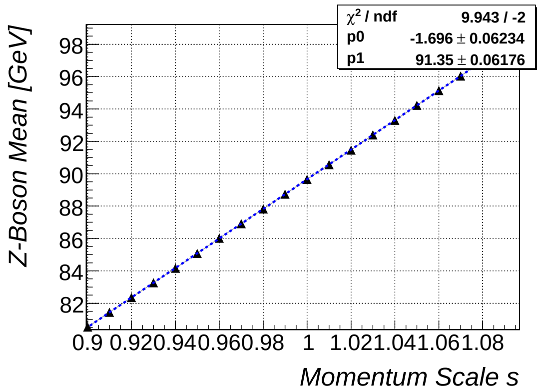

Figure 37: Expected mean of Z boson mass vs. the momentum scale s.

where c_μ is the charge of the muon, i.e. the shift on the momentum scale is symmetric for both cases. This is correct to first order approximation, but the momentum scales must be determined independently for positive and negative muons in second order. The shift on the momentum scale leads to a linear dependence with the measured mean of the reconstructed Z boson mass distribution (See FIG. 37). The momentum scale changes the Z bosons mass from two muons reconstructed in tower i and j as follows

$$M_{Z,ij}^{scale} = \sqrt{2 \cdot p_{T,1}^{scaled} p_{T,2}^{scaled} \cdot (\cosh(\Delta\eta) - \cos(\Delta\Phi))} = M_{Z,ij}\sqrt{(1+s_i^{\pm})(1+s_j^{\pm})} \tag{10}$$

where $M_{Z,ij}$ refers to the unscaled Z boson mass. This can be further approximated by

$$M_{Z,ij}^{scale} \approx M_{Z,ij}\left(1+\frac{s_i^{\pm}+s_j^{\pm}}{2}\right) \tag{11}$$

The momentum scales values of s_i and s_j can be determined by maximizing the negative likelihood function

$$-\ln L = \sum_{i,j=1}^{i=N,j=N} -\ln P\left(\frac{M_k}{1+\frac{s_i^{\pm}+s_j^{\pm}}{2}}\right) \tag{12}$$

where the function P gives the probability for a certain Z boson mass peek. The maximization can be performend with a χ^2-fit algorithm program like *Minuit*. With this method, the momentum scales s_i are determined for each tower in such a way that the measured Z boson mass is reproduced by the Monte Carlo simulation, which scales the simulated transverse momenta with the corresponding scaling factors.

In a final step, one has to relate Equation 7 with Equation 8. The impact of different values for Δs on the reconstructed muon momenta is studied within a Monte Carlo simulation. The value of Δs which reproduces the measured scaling factors s_i^+ and s_i^- is considered to be the net sagitta shift of the chosen tower.

This method is statistically limited by the precision with which the mean of the reconstructed Z boson mass distribution can be determined for each tower FIG. 39 illustrates the precision of measured mean value of the reconstructed Z boson mass distribution as a function of the number of selected events. To

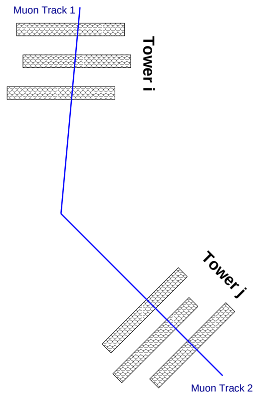

Figure 38: Illustration of two misaligned towers and two muon tracks from a Z boson decay.

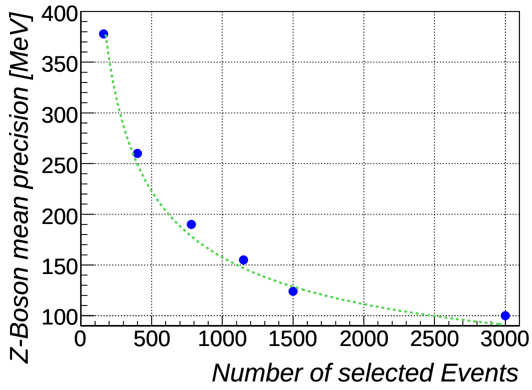

Figure 39: Precision of the measured mean of the reconstructed Z boson mass distribution vs. number of selected events.

reach a precision for the net sagitta value Δs of $100\mu m$, on the order of 400 muons with the same charge per tower, resulting from a Z boson decay, have to be selected and analyzed[12)]. This corresponds to an integrated luminosity of roughly 100 pb^{-1}, assuming a signal cross-section of 1495 pb, to achieve relative alignment of the Muon Spectrometer. Therefore the method will not be applicable for the first days of the ATLAS experiment, but might be used during the high luminosity phase for a daily cross-check.

It should be noted, that these are only the expected statistical limitations. Systematic uncertainties arising from the final state radiation of muons, energy loss in the calorimeter and imperfect magnetic field calculations and have not been considered in this discussion.

Acknowledgments

We especially thank C.Guyot, D.Levin, T.Liss, and R.Stroehmer for fruitful discussions and ideas regarding this study.

References

[1] ATLAS Collaboration, "*ATLAS Detector Design Report*", CERN/LHCC/99-14/15 (1997).

[2] ATLAS Collaboration, "*Muon Spectrometer Technical Design Report*", CERN/LHCC/99-14/15 (1997).

[3] K. A. Assamagan *et al. Final Report of the ATLAS AOD/ESD Definition Task Force*, ATLAS Internal note, ATLAS-SOFT-2004-006, December 2004.

[4] Boisvert, V; Calafiura, P; George, S; Polesello, G; Rajagopalan, S; Rousseau, D. *Final Report of the ATLAS Reconstruction Task Force* , ATL-SOFT-2003-010

[5] MUONBOY Web Page `http://atlas-samusog.web.cern.ch/atlas-samusog/muonboy/Muonboy.htm`.

[12)] As a rule of thumb, a 50 GeV-track corresponds to a sagitta of $1cm$.

[6] M. Virchaux *et al. Muonbox: a full 3D tracking programme for Muon reconstruction in the ATLAS Spectrometer*, ATL-MUON-97-198.

[7] http://atlas-samusog.web.cern.ch/atlas-samusog/muonboy/DocPublishedTexts/phytdr.staco.pdf

[8] M.Obermaier, Diploma thesis ”Integration of calibration and alignment procedures for the reconstruction of muons in the ATLAS experiment” , LMU Munich, GERMANY (2005)

[9] S.Kotov, ”Alignment of ATLAS Muon Chambers with Tracks”, (http://wwwatlas.mppmu.mpg.de/atlas_mdt/subpages/fig/talks_and_papers/MuonTrkAlign_Jun06.pdf), June 2006, ATLAS Muon Chamber Calibration Workshop, Rome, Italy, (2006)

[10] M.Schott, ”Study of the Sagitta Resolution of MDT-Chambers”, March 2006, ATL-MUON-PUB-2006-010, CERN (2006)

[11] J.Schmaler, Diploma thesis ”Track-based Alignment of the ATLAS Muon Spectrometer”, wwwatlas.mppmu.mpg.de/atlas_mdt/subpages/fig/talks_and_papers/JSchmaler_Diplomarbeit_2007.pdf, March 2007, MPI Munich, GERMANY (2007).